

# Modern imaging in Cushing's disease

\*WA Bashari<sup>1</sup>, \*D Gillett<sup>1,2</sup>, J MacFarlane<sup>1</sup>, AS Powlson<sup>1</sup>, AG Koliass<sup>3,4</sup>, R Mannion<sup>4</sup>, DJ Scoffings<sup>5</sup>, IA Mendichovszky<sup>2,5</sup>, J Jones<sup>5</sup>, HK Cheow<sup>2,5</sup>, O Koulouri<sup>1</sup>, M Gurnell<sup>1</sup>

Cambridge Endocrine Molecular Imaging Group, <sup>1</sup>Metabolic Research Laboratories, Wellcome–MRC Institute of Metabolic Science, and Departments of <sup>2</sup>Nuclear Medicine and <sup>3</sup>Neurosurgery, University of Cambridge and National Institute for Health Research Cambridge Biomedical Research Centre, Addenbrooke's Hospital, Cambridge Biomedical Campus, Cambridge, UK, CB2 0QQ.  
Departments of <sup>4</sup>Neurosurgery and <sup>5</sup>Radiology, Addenbrooke's Hospital, Cambridge Biomedical Campus, Cambridge, UK, CB2 0QQ.

**Corresponding author:** Professor Mark Gurnell, Wellcome–MRC Institute of Metabolic Science, University of Cambridge and National Institute for Health Research Cambridge Biomedical Research Centre, Addenbrooke's Hospital, Cambridge Biomedical Campus, Cambridge, UK, CB2 0QQ  
Email: mg299@medschl.cam.ac.uk

\* Denotes equal contribution

**Key words:** pituitary Cushing's, MRI, molecular / functional imaging, PET

**Running title:** Imaging in Cushing's Disease

**Word Count:** Text 1010 (excluding abstract); Figures 1

30 **Abstract**

31

32 Management of Cushing's disease is informed by dedicated imaging of the sella and  
33 parasellar regions. Although magnetic resonance imaging (MRI) remains the investigation of  
34 choice, a significant proportion (30–50%) of corticotroph tumours are so small as to render  
35 MRI indeterminate or negative when using standard clinical sequences. In this context,  
36 alternative MR protocols [e.g. 3D gradient (recalled) echo (GRE), with acquisition of  
37 volumetric data] may allow detection of tumors that have not been previously visualized. The  
38 use of hybrid molecular imaging [e.g. <sup>11</sup>C-methionine positron emission tomography (Met-  
39 PET) coregistered with volumetric MRI] has also been proposed as an additional modality  
40 for localizing microadenomas.

41

42 **Introduction**

43

44 The sense of achievement that accompanies successful navigation of the first phase of  
45 investigation in Cushing's syndrome (CS) is often tempered by the knowledge that localizing  
46 the source in ACTH-dependent disease may represent an even greater challenge due to the  
47 occult nature of many corticotroph and neuroendocrine tumors [1,2]. However, help is at  
48 hand, with several recent advances in MRI, CT (computed tomography) and PET, facilitating  
49 the successful detection of tumors that may be only a few millimeters in diameter. Here, we  
50 outline a stepwise approach to modern imaging in suspected pituitary-dependent CS.

51

52 **Pituitary MRI**

53

54 Most corticotroph tumors are microadenomas (even 'picoadenomas') and many (up to 50%)  
55 are not readily visualized using lower field strength [1.5 Tesla (1.5T)] MRI, especially if  
56 acquired using 2–3 mm slice thickness with gaps between consecutive slices. A tiered  
57 approach to sellar and parasellar MRI is therefore recommended, with early onward referral  
58 to a pituitary tumor center of excellence (PTCoE), especially when initial MRI findings are  
59 inconclusive [1–3].

60

61 ***Step 1a: core protocol [conventional spin echo (SE) MRI]***

62 • Coronal and sagittal T1-weighted (T1w) SE pre- and post-gadolinium

63 • Coronal T2w fast (turbo) spin echo (FSE/TSE)

64 Both sequences should be acquired with 2 (maximum 3) mm slice thickness and minimal

65 slice spacing, using 3T MRI [1,2,4]. For corticotroph macroadenomas (~10-20%) of all

66 corticotroph tumors, T2w sequences can provide useful information regarding the potential

67 invasion of adjacent parasellar structures and may also reveal a micro- or macrocystic  
68 appearance [1,2].

69

### 70 **Step 1b: recommended supplementary sequences**

71 If the core protocol does not identify a macroadenoma or obvious microadenoma, consider  
72 proceeding immediately (ideally in the same session) to:

- 73 • T1w gadolinium enhanced 3D-spoiled gradient (recalled) echo (3D-SGE/3D-GRE) MRI:
  - 74 – this allows volumetric (1 mm slice thickness) data acquisition, to provide better soft
  - 75 tissue contrast and improved detection of smaller lesions
  - 76 – and has been reported to localize up to 80–90% of corticotroph tumors [5,6]
- 77 • T1w gadolinium-enhanced dynamic MRI (dMRI):
  - 78 – which involves repeated data acquisitions every 10–20 s over 1–2 min, commencing
  - 79 with contrast injection (microadenomas show delayed enhancement during early
  - 80 phase)
  - 81 – however, although Liu and colleagues recently reported a high positive predictive
  - 82 value when dMRI was combined with high dose dexamethasone suppression testing
  - 83 [7], several groups have suggested that dMRI is inferior to SGE/GRE MRI and
  - 84 frequently yields false positive findings [1,2,6].

85

### 86 **Step 2: optional supplementary sequences / magnetic field strength**

87 When doubt remains as to the location of a corticotroph microadenoma, additional MR  
88 sequences or a higher magnetic field strength may be considered [1,2]:

- 89 • Fluid-attenuated inversion recovery (FLAIR) with gadolinium enhancement
  - 90 – to detect delayed contrast washout in a microadenoma [8]
- 91 • Constructive interference in steady state (CISS)
  - 92 – a high spatial resolution fast T2w gradient echo sequence, which allows fast
  - 93 acquisition times, high signal-to-noise ratio, and improved contrast-to-noise ratio [9]
- 94 • Isotropic 3D-fast (turbo) SE (e.g. *SPACE*, *Cube*, *VISTA*, *isoFSE*, *3D MVOX*)
  - 95 – which produces high resolution 3D images (with features of T1w, T2w and proton
  - 96 density MRI) [10]
- 97 • ultra-high field (7T) MRI

98

99 Whichever sequences are deployed, access to an expert neuroradiologist, supported by a  
100 specialist pituitary multidisciplinary team, is critical to maximizing the chance of localizing the  
101 causative lesion, whilst avoiding false attributions to artifacts or incidental lesions [2].

102

103 **Pituitary PET**

104 Even in centers with access to the full range of MR sequences, structural imaging may  
105 return indeterminate or negative results. The adoption of higher resolution techniques also  
106 increases the chance of detecting incidental lesions. In these contexts, molecular  
107 (functional) imaging can confirm or refute the site of a suspected microadenoma or reveal a  
108 previously unsuspected abnormality. Several radioligands have been used with varying  
109 degrees of success and are summarized here.

110

111 **<sup>11</sup>C-methionine PET (Met-PET)**

112 The introduction of hybrid imaging techniques [Met-PET/MR or Met-PET/CT coregistered  
113 with volumetric MRI (Met-PET/MR<sup>CR</sup>)] has allowed several groups to demonstrate the utility  
114 of combining anatomical and functional imaging with <sup>11</sup>C-methionine to localize small  
115 corticotroph adenomas [11–13]. This approach has been successfully used in both *de novo*  
116 and recurrent disease [13], and the development of enhanced image analysis tools, together  
117 with algorithms for 3D reconstruction and sellar profiling, offer the potential to further  
118 increase confidence in localizing very small tumors (Fig. 1).

119

120 ***Insert figure 1 here***

121

122 **<sup>18</sup>F-FET PET**

123 A key limitation of Met-PET is the short half-life (~20 min) of <sup>11</sup>C-methionine, which restricts  
124 its use to centers with an on-site cyclotron. In contrast, <sup>18</sup>F-fluoroethyl-tyrosine (FET) with its  
125 longer half-life (~110 min) can be synthesized and then transported to off-site centers. Both  
126 methionine and fluoroethyltyrosine are taken up at sites of peptide synthesis, possibly via  
127 the same L-type amino acid transporter (LAT1). To date, only a small number of patients  
128 with Cushing's disease have been imaged using <sup>18</sup>F-FET-PET/MR, but initial findings  
129 suggest a high predictive value for localizing corticotroph microadenomas [12].

130

131 **<sup>18</sup>F-FDG PET**

132 Although <sup>18</sup>F-fluorodeoxyglucose (<sup>18</sup>F-FDG) shares the benefits of a longer half-life and is  
133 more widely available, studies of <sup>18</sup>F-FDG PET in Cushing's disease have proved largely  
134 disappointing, with no clear benefits over conventional MRI in most published series.  
135 However, Boyle and colleagues have proposed that prior corticotropin releasing hormone  
136 (CRH) injection may increase the sensitivity of <sup>18</sup>F-FDG PET in Cushing's disease [14].

137

138 **<sup>68</sup>Ga(-DOTA)-CRH PET**

139 Recognizing that most corticotroph adenomas express CRH receptors (CRH-1R), Walia and  
140 colleagues observed that conjugation of <sup>68</sup>Ga-DOTA to CRH (<sup>68</sup>Ga-CRH) yields a PET ligand  
141 with apparent high sensitivity and specificity for the detection of ACTH-secreting pituitary  
142 adenomas [15]. However, importantly, only 10 of 24 subjects had adenomas <6 mm in size  
143 and in only 4 subjects was a lesion not visualized on MRI [15].

144

#### 145 ***<sup>68</sup>Ga(-DOTA)-SSTR PET***

146 Although corticotroph adenomas can express somatostatin receptor (SSTR) subtypes 2A, 3  
147 and 5, the use of <sup>68</sup>Ga-labelled SSTR ligands is largely reserved for the localization of  
148 neuroendocrine tumors (NETs) in the ectopic ACTH syndrome [1].

149

#### 150 **Conclusions**

151 As set out in the recent Pituitary Society guideline update [3], MRI remains the imaging  
152 modality of choice for the localization of ACTH-secreting pituitary adenomas and, when  
153 conducted in a specialist unit with access to the full complement of sequences, will identify  
154 the causative lesion in many cases. However, when uncertainty persists, molecular PET  
155 imaging may allow the causative lesion to be located.

156

157 **Declarations**

158

159 **Funding declaration**

160 W Bashari, J MacFarlane, A Koliass, O Koulouri and M Gurnell are supported by the NIHR  
161 Cambridge Biomedical Research Center (BRC-1215-20014). A Koliass is supported by the  
162 Wellcome Trust Institutional Strategic Support Fund, University of Cambridge.

163

164 **Author information**

165

166 **Affiliations**

167

168 **Cambridge Endocrine Molecular Imaging Group, Metabolic Research Laboratories,**  
169 **Wellcome–MRC Institute of Metabolic Science, University of Cambridge and National**  
170 **Institute for Health Research Cambridge Biomedical Research Centre, Addenbrooke's**  
171 **Hospital, Cambridge Biomedical Campus, Cambridge, UK, CB2 0QQ**

172 WA Bashari, D Gillett, J MacFarlane, AS Powlson, AG Koliass, O Koulouri and M Gurnell

173

174 **Cambridge Endocrine Molecular Imaging Group, Department of Nuclear Medicine,**  
175 **University of Cambridge and National Institute for Health Research Cambridge**  
176 **Biomedical Research Centre, Addenbrooke's Hospital, Cambridge Biomedical**  
177 **Campus, Cambridge, UK, CB2 0QQ**

178 D Gillett, IA Mendichovszky and HK Cheow

179

180 **Department of Neurosurgery, Addenbrooke's Hospital, Cambridge Biomedical**  
181 **Campus, Cambridge, UK, CB2 0QQ**

182 AG Koliass and R Mannion

183

184 **Department of Radiology, Addenbrooke's Hospital, Cambridge Biomedical Campus,**  
185 **Cambridge, UK, CB2 0QQ**

186 DJ Scoffings, IA Mendichovszky, J Jones and HK Cheow

187

188 **Contributions**

189 All authors contributed equally and reviewed the final manuscript before submission

190 **References**

- 191 [1] Senanayake R, Gillett D, MacFarlane J, Van de Meulen M, Powlson A, Koulouri O, et  
192 al. New types of localization methods for adrenocorticotrophic hormone-dependent  
193 Cushing's syndrome. *Best Pract Res Clin Endocrinol Metab* 2021;35.  
194 <https://doi.org/10.1016/j.beem.2021.101513>.
- 195 [2] Bonneville J, Potorac I, Petrossians P, Tshibanda L, Beckers A. Pituitary MRI in  
196 Cushing's disease - an update. *J Neuroendocrinol* 2022:e13123.  
197 <https://doi.org/10.1111/jne.13123>.
- 198 [3] Fleseriu M, Auchus R, Bancos I, Ben-Shlomo A, Bertherat J, Biermasz NR, et al.  
199 Consensus on diagnosis and management of Cushing's disease: a guideline update.  
200 *Lancet Diabetes Endocrinol* 2021;9:847–75. [https://doi.org/10.1016/S2213-](https://doi.org/10.1016/S2213-8587(21)00235-7)  
201 [8587\(21\)00235-7](https://doi.org/10.1016/S2213-8587(21)00235-7).
- 202 [4] Erickson D, Erickson B, Watson R, Patton A, Atkinson J, Meyer F, et al. 3 Tesla  
203 magnetic resonance imaging with and without corticotropin releasing hormone  
204 stimulation for the detection of microadenomas in Cushing's syndrome. *Clin*  
205 *Endocrinol (Oxf)* 2010;72:793–9. <https://doi.org/10.1111/j.1365-2265.2009.03723.x>.
- 206 [5] Kasaliwal R, Sankhe SS, Lila AR, Budyal SR, Jagtap VS, Sarathi V, et al. Volume  
207 interpolated 3D-spoiled gradient echo sequence is better than dynamic contrast spin  
208 echo sequence for MRI detection of corticotropin secreting pituitary microadenomas.  
209 *Clin Endocrinol (Oxf)* 2013;78:825–30. <https://doi.org/10.1111/cen.12069>.
- 210 [6] Grober Y, Grober H, Wintermark M, Jane JA, Oldfield EH. Comparison of MRI  
211 techniques for detecting microadenomas in Cushing's disease. *J Neurosurg*  
212 2018;128:1051–7. <https://doi.org/10.3171/2017.3.JNS163122>.
- 213 [7] Liu Z, Zhang X, Wang Z, You H, Li M, Feng F, et al. High positive predictive value of  
214 the combined pituitary dynamic enhanced MRI and high-dose dexamethasone  
215 suppression tests in the diagnosis of Cushing's disease bypassing bilateral inferior  
216 petrosal sinus sampling. *Sci Rep* 2020;10:14694. [https://doi.org/10.1038/s41598-020-](https://doi.org/10.1038/s41598-020-71628-0)  
217 [71628-0](https://doi.org/10.1038/s41598-020-71628-0).
- 218 [8] Chatain GP, Patronas N, Smirniotopoulos JG, Piazza M, Benzo S, Ray-Chaudhury A,  
219 et al. Potential utility of FLAIR in MRI-negative Cushing's disease. *J Neurosurg*  
220 2018;129:620–8. <https://doi.org/10.3171/2017.4.JNS17234>.
- 221 [9] Lang M, Habboub G, Moon D, Bandyopadhyay A, Silva D, Kennedy L, et al.  
222 Comparison of Constructive Interference in Steady-State and T1-Weighted MRI  
223 Sequence at Detecting Pituitary Adenomas in Cushing's Disease Patients. *J Neurol*  
224 *Surgery, Part B Skull Base* 2018;79:593–8. <https://doi.org/10.1055/s-0038-1642032>.
- 225 [10] Wu Y, Cai Y, Rui W, Tang Y, Yang Z, He M, et al. Contrast-enhanced 3D-T2-  
226 weighted SPACE sequence for MRI detection and localization of adrenocorticotropin

- 227 (ACTH)-secreting pituitary microadenomas. *Clin Endocrinol (Oxf)* 2022;96:578–88.  
228 <https://doi.org/10.1111/cen.14574>.
- 229 [11] Ikeda H, Abe T, Watanabe K. Usefulness of composite methionine-positron emission  
230 tomography/3.0-tesla magnetic resonance imaging to detect the localization and  
231 extent of early-stage Cushing adenoma. *J Neurosurg* 2010;112:750–5.  
232 <https://doi.org/10.3171/2009.7.JNS09285>.
- 233 [12] Berkmann S, Roethlisberger M, Mueller B, Christ-Crain M, Mariani L, Nitzsche E, et  
234 al. Selective resection of cushing microadenoma guided by preoperative hybrid 18-  
235 fluoroethyl-L-tyrosine and 11-C-methionine PET/MRI. *Pituitary* 2021;24:878–86.  
236 <https://doi.org/10.1007/s11102-021-01160-5>.
- 237 [13] Koulouri O, Steuwe A, Gillett D, Hoole AC, Powlson AS, Donnelly NA, et al. A role for  
238 11C-methionine PET imaging in ACTH-dependent Cushing’s syndrome. *Eur J*  
239 *Endocrinol* 2015;173:M107-20. <https://doi.org/10.1530/EJE-15-0616>.
- 240 [14] Boyle J, Patronas NJ, Smirniotopoulos J, Herscovitch P, Dieckman W, Millo C, et al.  
241 CRH stimulation improves 18F-FDG-PET detection of pituitary adenomas in  
242 Cushing’s disease. *Endocrine* 2019;65:155–65. [https://doi.org/10.1007/s12020-019-](https://doi.org/10.1007/s12020-019-01944-7)  
243 [01944-7](https://doi.org/10.1007/s12020-019-01944-7).
- 244 [15] Walia R, Gupta R, Bhansali A, Pivonello R, Kumar R, Singh H, et al. Molecular  
245 Imaging Targeting Corticotropin-releasing Hormone Receptor for Corticotropinoma: A  
246 Changing Paradigm. *J Clin Endocrinol Metab* 2021;106:e1816–26.  
247 <https://doi.org/10.1210/clinem/dgaa755>.
- 248

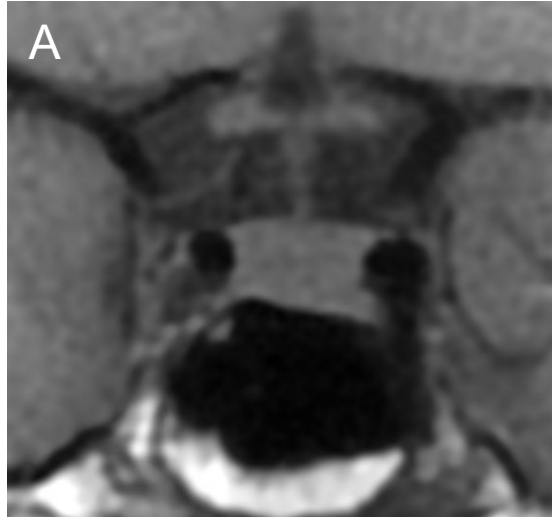


249 **Figure legend**

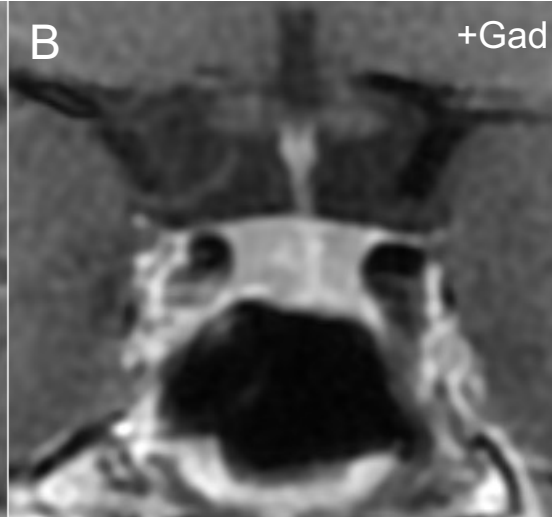
250

251 **Fig. 1 MRI and Met-PET findings with 3D reconstruction of the sella and parasellar**  
252 **regions in a patient with ACTH-dependent Cushing's syndrome. A–C, Pre- and post-**  
253 **contrast coronal T1w SE MRI (A–B) and FSPGR (volumetric) MRI (C) demonstrate equivocal**  
254 **appearances, with subtle deviation of the infundibulum to the left, but minor downward sloping**  
255 **of the floor of the sella on the left side. No discrete microadenoma is readily visualized. D,**  
256 **Met-PET/MR<sup>CR</sup> reveals both central (white arrow) and right-sided (yellow arrow) radiotracer**  
257 **uptake in the gland. E–F, 3D reconstructed images, combining PET, CT and FSPGR MRI**  
258 **datasets, allows appreciation of the location of the tumor (yellow) with respect to the normal**  
259 **gland (turquoise) and other adjacent structures including the intracavernous carotid arteries**  
260 **(red) and optic chiasm (green). G, Profiling of <sup>11</sup>C-methionine uptake across the sella reveals**  
261 **two peaks consistent with uptake by normal gland and a corticotroph microadenoma. At**  
262 **transsphenoidal surgery, a microadenoma was resected from the right side of the gland and**  
263 **confirmed histologically to be a corticotroph adenoma. Postoperatively the patient achieved**  
264 **complete clinical and biochemical remission and remains eupituitary. Key:** CT, computed  
265 tomography; FSPGR, fast spoiled gradient recalled echo; Gad, gadolinium; Met-PET/MR<sup>CR</sup>,  
266 <sup>11</sup>C-methionine PET-CT coregistered with volumetric (FSPGR) MRI; MRI, magnetic  
267 resonance imaging; PET, positron emission tomography; SE, spin echo; T1w, T1-weighted.

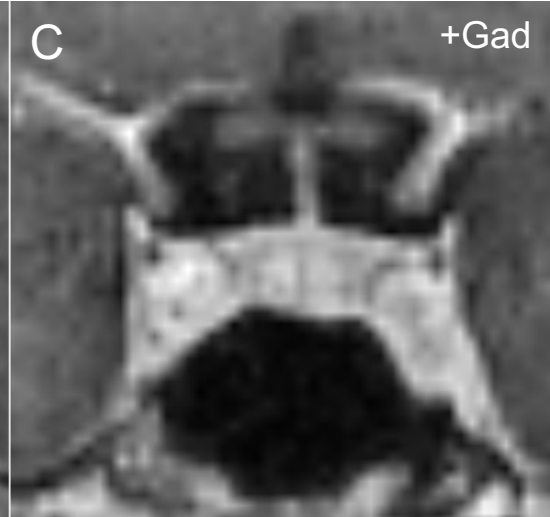
T1w SE MRI  
(pre-contrast)



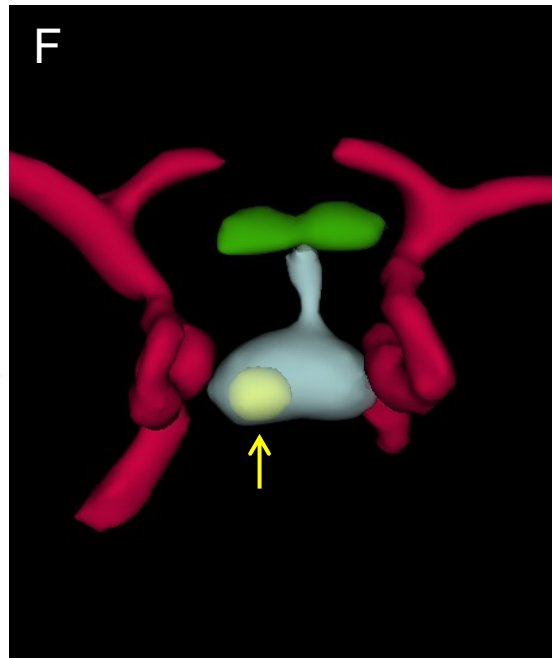
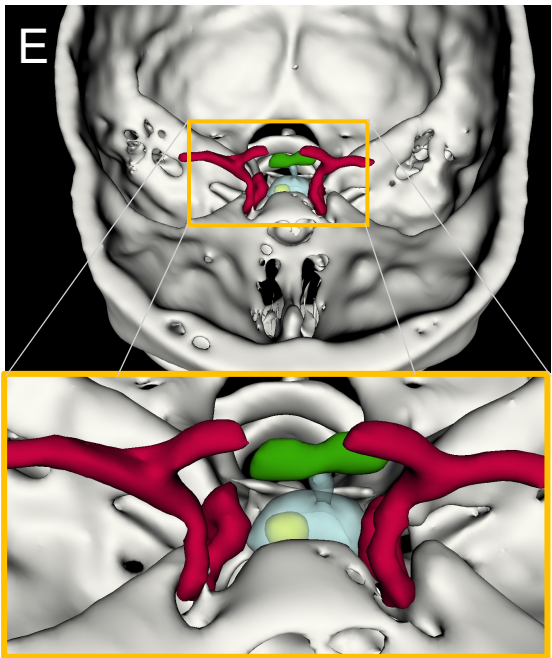
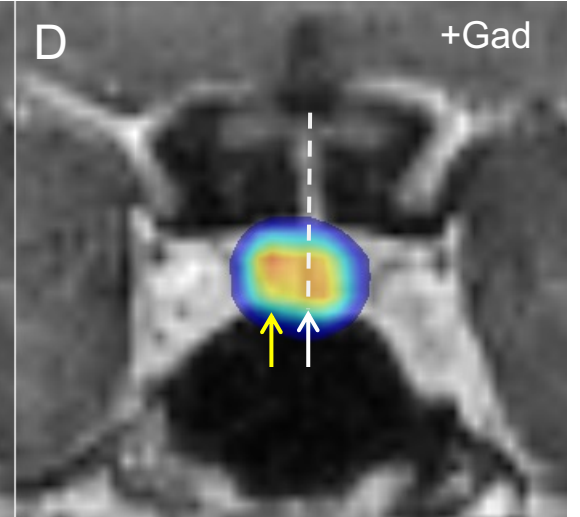
T1w SE MRI  
(post-contrast)



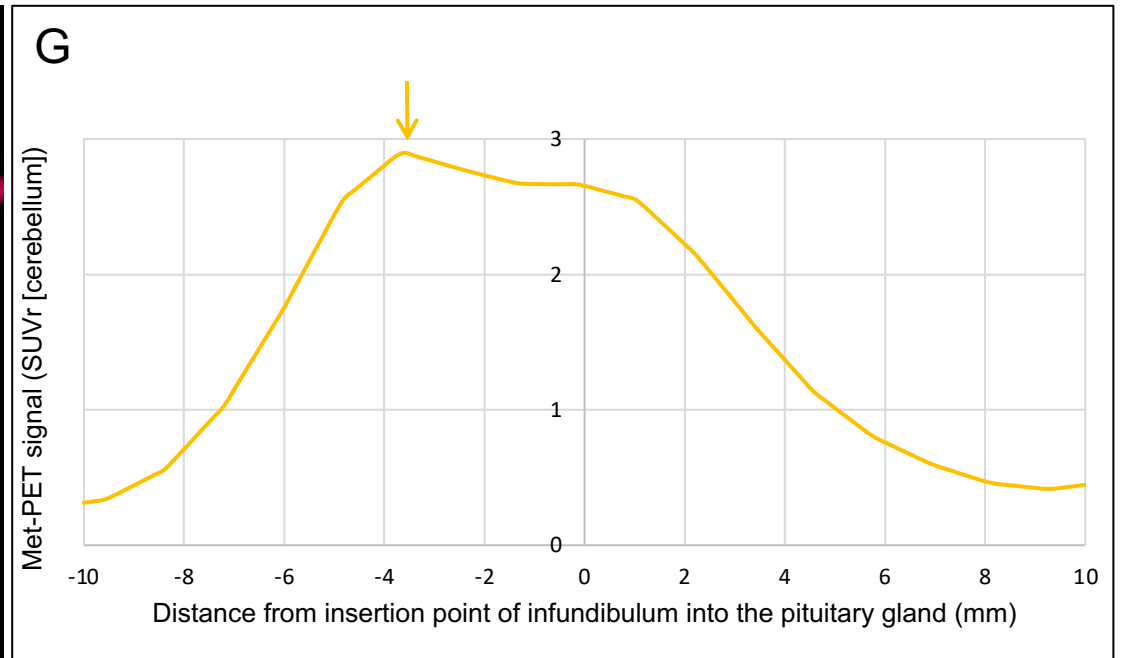
FSPGR MRI  
(post-contrast)



Met-PET/MR<sup>CR</sup>



3D reconstructions



Met-PET signal profile